Slag-metal interactions in the FeMn tapping process: Interfacial properties and wetting

Sergey Bublik, Sarina Bao, Merete Tangstad, Kristian Etienne Einarsrud

FeMn-alloys are produced by transforming ore and carbon materials into FeMn and slag at high temperatures in a furnace. Entrainment of FeMn in slag during tapping reduces the yield. Entrainment and subsequent separation are strongly influenced by slag-metal interfacial properties. In the current work, interfacial properties, including the contact angle, in the FeMn-slag graphite system have been investigated using the sessile drop technique at temperatures above 1573 K. Two experimental configurations are proposed: (a) slag and metal placed beside each other on graphite; and (b) slag placed on top of the metal layer, which is in contact with graphite. Results demonstrate that the contact angle between slag and metal is 55-60° at temperatures from 1583 to 1623 K at slag-metal weight ratio around 0.25. In addition, wetting properties are considerably influenced by the variation of slag-metal weight ratio in the range from 0.25 to 1.50 and only marginally by temperature.

I. INTRODUCTION

At the present time, the production of ferromanganese and other types of ferroalloys is consistently growing, which is partly caused by the increased demand for steel and these alloys[1–3]. High carbon FeMn production (78 per cent Mn, 15 per cent Fe, 7 per cent C) reached the level of 4.2 million t in 2017[4]. FeMn and most of the ferroalloys (SiMn, FeSi, FeCr) are produced in submerged arc furnaces (SAF) during high-temperature reduction of the oxide raw materials by carbon (coke, anthracite, charcoal). In addition to the ferroalloy, a significant amount of slag is generated[5]. The slag-to-metal ratio depends upon the quality of raw materials and operational conditions: for FeMn production, the slag-to-metal ratio varies from 0.60 to 1.22[6]. There are several methods for tapping of products from the SAF, such as combined metal and slag tapping, dedicated metal-slag tapping and slag-only tapping[7]. In the ferroalloy production industry, the combined method is typically used, where both slag and metal are tapped periodically every 2-3 hours. The taphole can be changed in order to prevent operational difficulties and to stabilize the molten bath level[8]. As a consequence, slag and metal must be separated after tapping to obtain the required quality of FeMn. Typically, this is performed in a cascade of ladles, where the separation takes place due to the density difference between products, and liquid slag overflows to the following ladles. The slag overflow, nevertheless, entrains unseparated FeMn droplets, resulting in metal losses and thereby decreasing the process efficiency. The entrainment of the molten FeMn droplets by the slag phase is greatly affected by interfacial phenomena, which are mainly determined by the interfacial tension[9–12].

The measurement of the interfacial tension between two molten phases is extremely challenging due to the high temperature and the complexity of phase composition. Specifically, the presence of dissolved surface active elements (oxygen, sulphur) at the interface between slag and metal could

SERGEY BUBLIK, MERETE TANGSTAD and KRISTIAN ETIENNE EINARSRUD are with the Department of Materials Science and Engineering, Norwegian University of Science and Technology (NTNU), 7941 Trondheim, Norway. Contact e-mail: sergey.bublik@ntnu.no

SARINA BAO is with the Department of Metal Production and Processing, SINTEF Industry, 7941 Trondheim, Norway

considerably modify the interfacial tension[13,14]. Moreover, available methods for the determination the interfacial tension are complicated and do not allow to investigate interfacial phenomena with stable and reproducible results.

In the present work, the interfacial properties between high carbon FeMn and FeMn slag (CaO-MnO-SiO_2-MgO-Al_2O_3) have been studied using the sessile drop technique. Two different experimental methods are presented and discussed, aiming to determine their applicability to the current system.

II. EXPERIMENTAL PROCEDURE

A. Materials preparation

FeMn slag and HC FeMn compositions and densities were selected corresponding to that of industrial products, which are presented in **Table I**. Both FeMn and slag were made from pure powder materials. The purity of powders and the weight of powders, are shown in **Table II**.

The powders were mixed and melted in a graphite crucible in a graphite tube furnace in argon at 1773 K. The obtained product after melting and solidification was then removed from the crucible and crushed.

It is noteworthy to mention that carbon materials were not added during the mixing of powders for HC FeMn due to the carbon available from the graphite crucible.

Table I. Chemical composition of the industrial FeMn and FeMn slag.

Material	Chemical composition, wt. %[15]								Density, kg/m³[16]
	Mn	Fe	C	CaO	MnO	SiO_2	MgO	Al_2O_3	
FeMn	78	15	7	-	-	-	-	-	7200
FeMn slag	-	-	-	23	38	23	6	10	3500

Table II. The purity and the weight of powders for the mixing.

Material	Purity, %						
	Mn	Fe	CaO	MnO	SiO_2	MgO	Al_2O_3
Powder	99.99	98.00	98.00	99.00	99.99	98.00	95.00 (5 % SiO_2)

Synthetic material	Weight of mixed powders, g								
	Mn	Fe	C	CaO	MnO	SiO_2	MgO	Al_2O_3	Total
HC FeMn	41.94	8.23	-	-	-	-	-	-	50.17
FeMn slag	-	-	-	11.73	19.19	11.24	3.06	5.26	50.48

B. Experimental Setup

In order to study the interfacial properties between synthetic FeMn slag and HC FeMn, the sessile drop technique was applied. The experimental equipment is illustrated schematically in **Fig. 1**.

Two experimental methods were made:

Method A – slag (15-125 mg) and FeMn (60-120 mg) placed beside each other on a graphite substrate (d = 1 cm);

Method B – slag (~60-90 mg) placed on the top of the FeMn layer (~300 mg), which is in contact with a graphite substrate (d = 1 cm).

Slag and FeMn pieces, as shown in **Fig. 2**, were located on a graphite substrate (ISO-88), which was cleaned by compressed air. Subsequently, the chamber of the sessile drop furnace was closed, evacuated, rapidly heated in argon atmosphere up to 1423 K in 3.75 minutes (300 K/min) and then heated up to 1623 K in 10 minutes (20 K/min). After reaching 1623 K, the furnace was turned off and samples cooled down. Thereafter the samples were cast in epoxy, sectioned in the centre and prepared for the electron microprobe analysis (EPMA) by wavelength-dispersive spectroscopy. The composition of slag and FeMn before and after the sessile drop test were measured in several points and then average composition of each phase was calculated. The experimental matrix for both methods is represented in **Table III**.

The chamber of the furnace was equipped with windows in order to allow a digital video camera (Sony XCD-SX910CR, Sony Corporation, Millersville, MD) with a telecentric lens (Navitar 1-50993D) to record images from the molten samples with the resolution of 1280x1024 pixels at one frame per second. This means three frames per degree of temperature increase from 1423 K and above.

The contact angles between different phases in method A were measured directly from the image using the image processing software (ImageJ[17]). Values for surface- and interfacial tension were not obtained for method A due to challenges in fitting regular shapes to the interfaces in question.

For method B, the interfacial and the surface tension were estimated from the contour of droplets during experiments in the sessile drop furnace using the axisymmetric drop shape analysis (ADSA)[18], which is based on the balance between surface, interfacial tension and external forces.

The figures after analysing the raw data were produced using a data visualization toolbox for MATLAB (Gramm[19]). The confidence bands for fitted lines are given by:

$$C = b \pm t\sqrt{S} \qquad [1]$$

where b are the coefficients produced by the fit, t is the value, which depends on the confidence level and is computed using the inverse of Student's t cumulative distribution function, S is a vector of the diagonal elements from the estimated covariance matrix of the coefficient estimates.

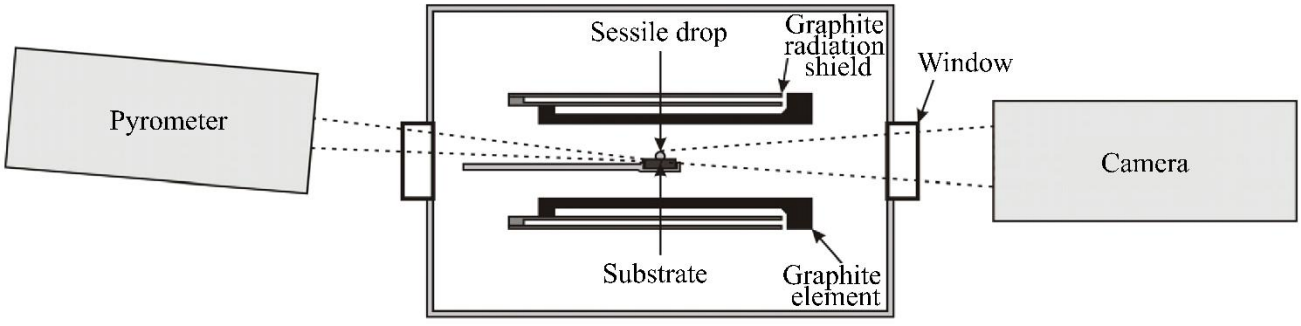

Fig. 1 – Schematic illustration of the sessile drop technique[20]

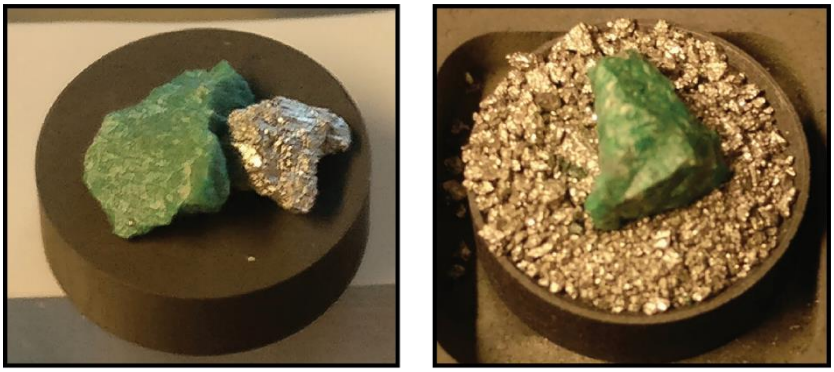

Method A Method B

Fig. 2 – Raw materials before experiments: A, slag and metal side by side on a graphite disk; B, slag on the metal layer in a graphite cup

Table III. The experimental matrix.

Experiment	Slag-to-metal weight ratio (S/M)		
	Average	Min	Max
Method A			
A1-A3	0.25	0.22	0.27
A4-A6	0.49	0.46	0.52
A7-A9	0.73	0.71	0.74
A10-A12	0.97	0.92	1.00
A13-A15	1.26	1.21	1.29
A16-A18	1.54	1.52	1.56
Method B			
B1-B3	0.19	0.18	0.20
B4-B6	0.28	0.26	0.29

III. RESULTS AND DISCUSSION

The changes in the droplets shape during melting are presented for both methods in **Fig. 3** and **Fig. 4**, respectively, together with a schematic view of relevant contact angles. The contact angles were defined geometrically as described below:

- slag-graphite ($\theta_{s\text{-}gr}$) is the angle formed by the tangent to the slag-graphite interface;
- metal-graphite ($\theta_{m\text{-}gr}$) is the angle formed by the tangent to the metal-graphite interface;
- slag-metal ($\theta_{m\text{-}gr}$) is the angle formed by two tangent lines from the contact point of slag and metal.

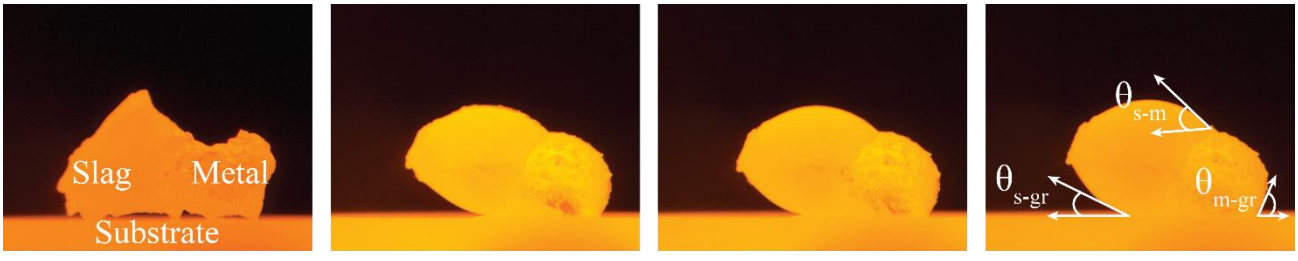

(a) (b) (c) (d)

Fig. 3 – Experiment A9, S/M = 0.73, melting of the slag (left) and FeMn (right): (a) samples before melting, T = 1473 K; (b) T = 1573 K; (c) T = 1598 K; (d) T = 1623 K. Relevant contact angles are indicated in frame (d).

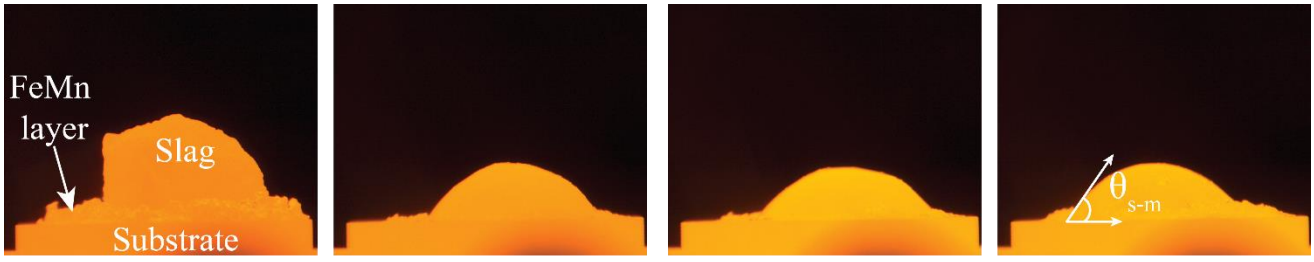

Fig. 4 – Experiment B4, S/M = 0.28, melting of slag placed on the FeMn layer: (a) slag before melting, T = 1473 K; (b) T = 1573 K; (c) T = 1598 K; (d) T = 1623 K. The relevant contact angle is indicated in frame (d).

A. Wetting according to the method A

Melting points of FeMn and slag were found to be 1533 K and 1563 K, respectively. In order to represent conditions relevant to the tapping process, contact angles were determined between 1583 and 1623 K. The rate of reduction increases at higher temperatures, thereby contributing to uncertainties.

Fig. 5(a) shows that the measured contact angle varies, depending on the interface and the slag-to-metal ratio in the range from 0.25 to 1.50. Values of the contact angle between metal-graphite and slag-graphite are more randomly distributed, resulting in low adjusted R-squared values (0.05 and 0.13, respectively). In contrast, values of the contact angle between slag-metal have higher adjusted R-squared value (0.60), indicating a larger dependence within the limits of the plotted linear model.

The apparent contact angle at the metal-graphite interface changes considerably with the slag-to-metal ratio due to the gravity effect, which become more substantial with increasing the volume of the slag droplet, while the volume of the FeMn droplet is fixed.

Below a certain value of the drop volume, the dominant forces are capillary terms and any gravity effects in the system can be ignored. However, with increasing droplet volumes, the gravity influence becomes more pronounced, which contributes to a stronger effect of gravity[21] and a change in the apparent interfacial (or surface) tension, which is determined by[22]:

$$a^2 = \frac{V}{l} = \frac{\sigma}{\Delta\rho g} \qquad [2]$$

where a is the capillary constant, V is the volume of raised liquid, l is the length of the capillary perimeter, σ is the interfacial or surface tension of the liquid, $\Delta\rho$ is the density difference between two phases, g is the gravity constant.

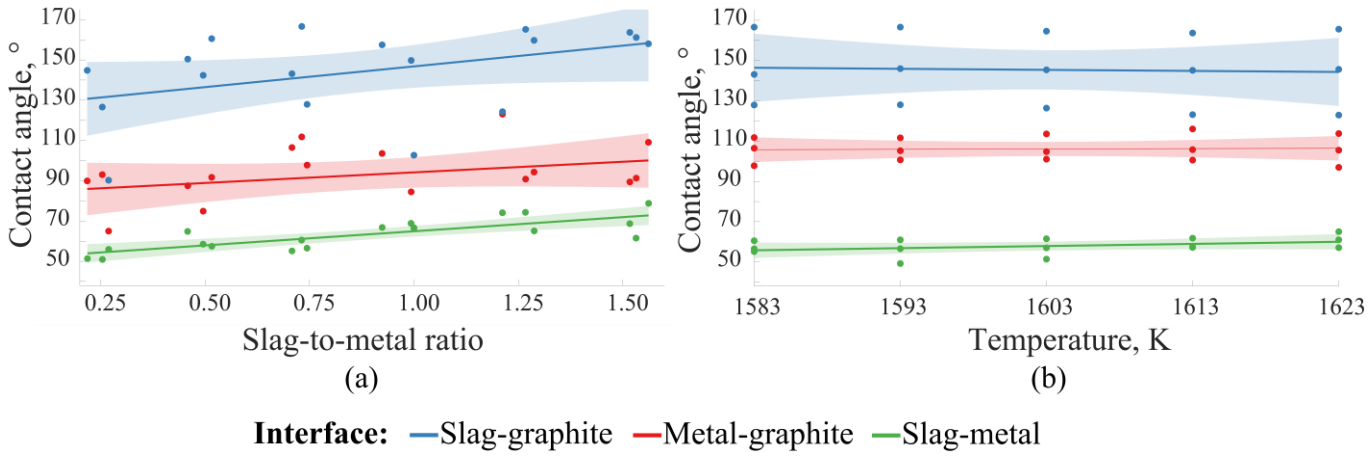

Fig. 5 – Experiments A1-A18: Measured contact angles and linear regression with 95 % confidence bands (lines and shaded areas): (a) at different slag-to-metal ratio at 1583 K, (b) at different temperature at S/M from 0.71 to 0.74.

The results of the contact angle at different temperatures and at fixed slag-to-metal ratio (close to 0.75) demonstrate that the effect of temperature in the range from 1583 to 1623 K is negligible (**Fig. 5(b)**). Values of the contact angle for different interfaces are:

- metal-graphite: 144.4–146.4°;
- slag-graphite: 105.8–106.5°;
- slag-metal: 55.8–60.0°.

B. Interfacial behaviour according to the method B

The apparent interfacial tension between slag and metal at the slag metal ratio from 0.18 to 0.29 is demonstrated in **Fig. 6(a)**. The value of the interfacial tension, calculated based on the ADSA approach, is 1.03–1.18 N/m when the slag-to-metal ratio is in the range from 0.18 to 0.21, while increasing the slag-to-metal ratio to 0.26–0.29 leads to the higher values of the interfacial tension (1.20–1.56 N/m).

In case of higher values of the slag-to-metal ratio, the apparent interfacial tension has higher values due to the gravity effect, which becomes more pronounced with increasing the slag volume when the volume of the FeMn layer is fixed. According to the **Eq. [2]**, higher volume results in higher values of the interfacial tension. Calvimontes[23] has shown that the interfacial properties can be greatly modified by the gravitational force, resulting in increased apparent wetting and considerably lower measured contact angles. As indicated in (**Fig. 6(b)Error! Reference source not found.**), the slag-Ar surface tension does not show a (statistically) significant influence from the slag-to-metal ratio, which is as expected as the curvature of the upper surface of the droplet is relatively straight forward to fit to an oblate. The mean value of the slag surface tension is found to be 1.14 N/m.

As presented in **Fig. 7**, both the interfacial and surface tension tend to slightly decrease as the temperature rises in the experimental range. Several studies[24–27] have shown a similar temperature dependence.

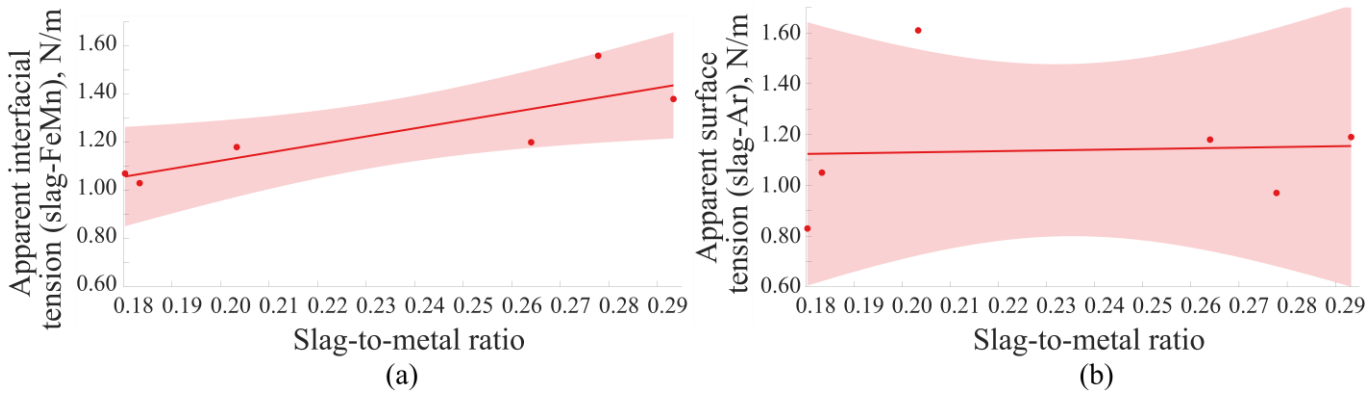

Fig. 6 – Experiments B1-B6: the interfacial tension between slag and metal (a) and the surface tension of slag in Ar (b) at different slag-to-metal ratio at 1583 K and linear regression with the 95 % confidence band (lines and the shaded areas).

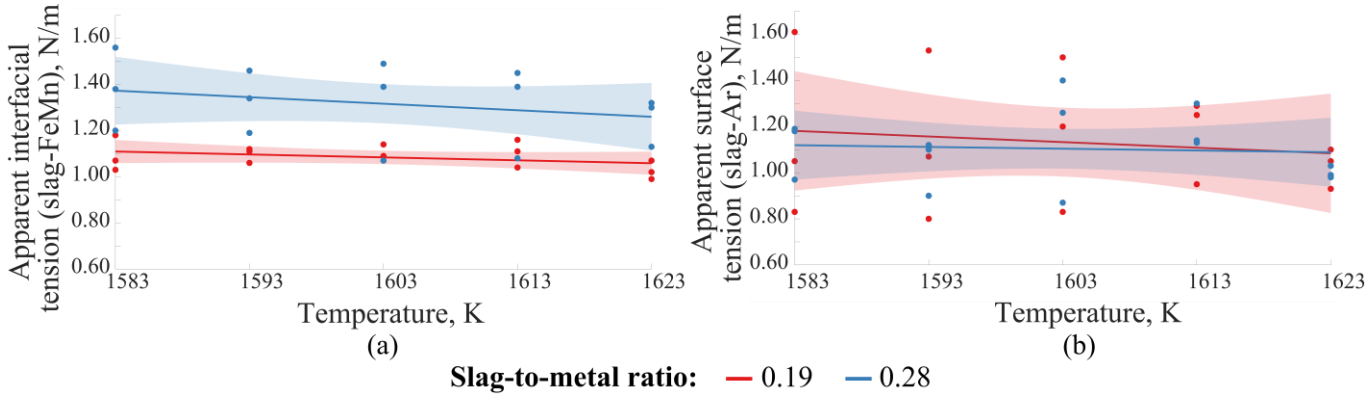

Fig. 7 – Experiments B1-B6: the interfacial tension between slag and metal (a) and the surface tension of slag in Ar (b) as a function of temperature and linear regression with the 95 % confidence bands (lines and shaded areas).

The apparent contact angle between slag and metal was found to be in the range of 43.3-64.6° for method B, determined by image analysis, in good correspondence with that found with method A.

C. EPMA of the raw materials and samples after the experiments

The EPMA images with 200 times magnification both for FeMn slag and FeMn after melting in the graphite crucible are presented in **Fig. 8**. The initial average chemical compositions of slag and FeMn are summarized in **Table IV**. Comparing to the **Table I**, we can see that the raw materials are close in composition to the industrial FeMn slag and FeMn. According to the Kim et al. (2003)[28] the carbon solubility in Mn-Fe melts (15 % Fe) at 1773 K is 7.5 %. The graphite crucible introduced expected amounts of carbon into the FeMn.

The results from the point analysis by EPMA (**Table V**) demonstrates that the slag contains two phases: the matrix and dendrites (MnO and MgO). **Fig. 8(b)** shows that FeMn consists of four different phases, the composition of which is demonstrated in **Table VI.**

Fig. 9(a) shows the slag phase of the sample after experiment in the sessile drop furnace using method B. The point analysis by EPMA (**Table VII**) illustrates that the slag matrix has the similar composition to the slag prior the experiment, while dendrites contain slightly higher MgO content (mean value of 12.5 %) and lower MnO content (mean value of 84.5 %).

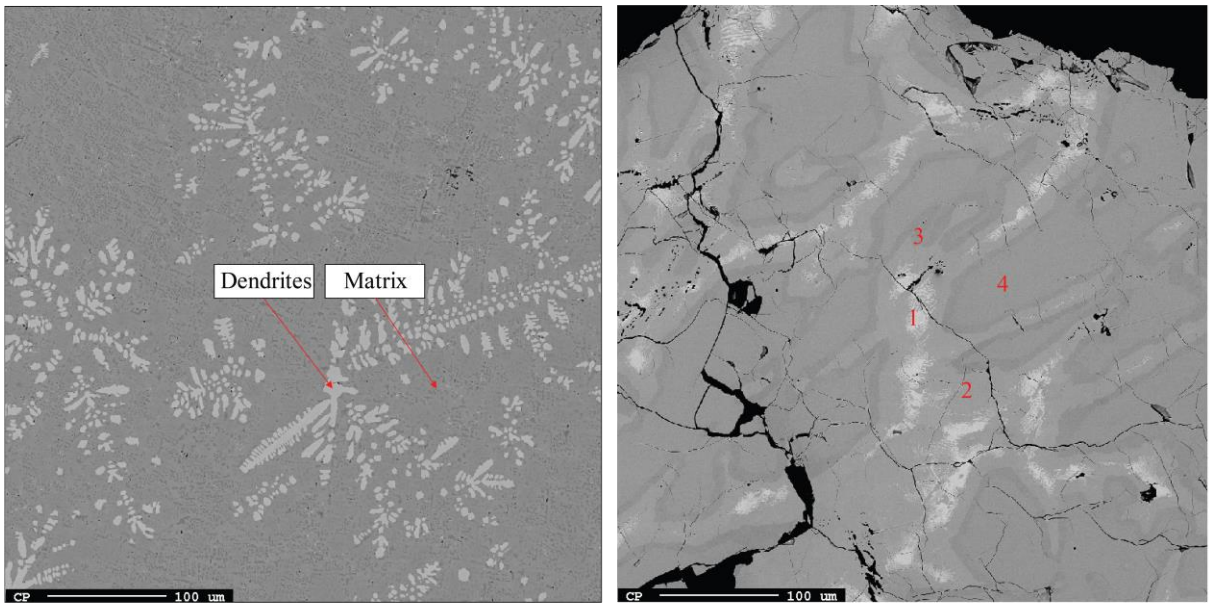

(a) (b)

Fig. 8 – EPMA image of FeMn slag (a) and FeMn (b) before the experiments.

Table IV. The average chemical composition of materials before the experiments in the sessile drop furnace.

Material	Average chemical composition, wt. %									
	Mn	**Fe**	**C**	**CaO**	**MnO**	**SiO_2**	**MgO**	**Al_2O_3**	**FeO**	**Total**
FeMn slag	-	-	-	22.7	35.2	23.0	5.6	10.5	0.1	97.1
FeMn	80.4	14.9	6.7	-	-	-	-	-	-	102.0

Table V. Chemical composition of slag phases, measured at different points.

Phase	Average chemical composition, wt. %						
	CaO	**MnO**	**SiO_2**	**MgO**	**Al_2O_3**	**FeO**	**Total**
Dendrites	1.5	87.1	0.0	8.8	0.4	0.2	97.9
Matrix	26.7	27.0	22.7	5.3	12.7	0.0	94.4

Table VI. Chemical composition of FeMn phases, measured at different points.

No.	Average chemical composition, wt. %			
	Mn	**Fe**	**C**	**Total**
1	75.5	28.0	2.8	106.3
2	79.0	18.4	5.6	103.1
3	80.0	15.0	6.3	101.3
4	79.6	14.4	6.4	100.5

However, it has been observed that the metal phase of the sample after experiment B6 (**Fig. 9(b)**) consist of only two phases, the chemical analysis of which is presented in **Table VIII**, compared to the FeMn sample before the experiment, which has four phases. This was found for all samples considered.

The interface between slag and FeMn is shown in **Fig. 9(c)**. As demonstrated, the slag penetrates the metal, resulting in a significant amount of slag inclusions near the interface. The point analysis of the inclusions, obtained from samples after experiments B1-B5, is presented in **Table IX**.

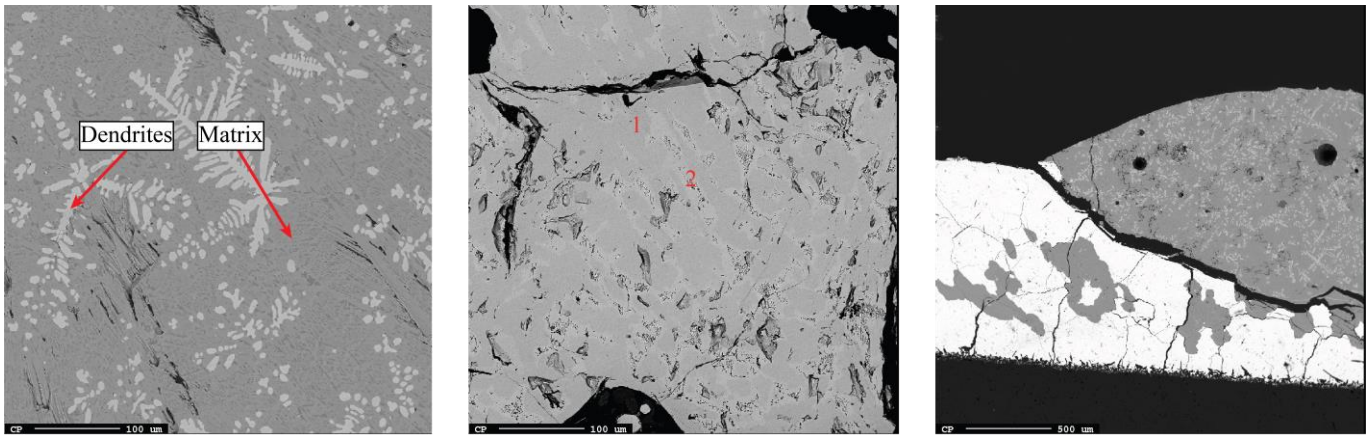

(a) (b) (c)

Fig. 9 – EPMA images of the sample after experiment B6: (a) slag phase, (b) metal phase, (c) the interface between slag and metal phase.

Table VII. Chemical composition of the slag phase of the sample after experiment B6.

No.	Average chemical composition, wt. %						
	CaO	MnO	SiO_2	MgO	Al_2O_3	FeO	Total
Dendrites	1.4	84.5	0.0	12.5	0.4	0.2	98.9
Matrix	26.0	28.8	24.3	5.2	11.2	0.1	95.5

Table VIII. Chemical composition of the metal phase of the sample after experiment B6.

No.	Average chemical composition, wt. %			
	Mn	Fe	C	Total
1	78.3	19.0	5.6	102.8
2	78.8	17.2	6.2	102.2

Table IX. Chemical composition of the slag inclusions in the metal phase.

Average chemical composition, wt. %						
CaO	MnO	SiO_2	MgO	Al_2O_3	FeO	Total
26.8	27.0	27.5	4.6	11.1	0.2	97.2

IV. CONCLUSIONS

Two methods for the measurement of the interfacial properties between FeMn and FeMn slag were studied in the sessile drop furnace at temperature from 1583 to 1623 K under Ar atmosphere. Both methods are suitable for the investigation of interfacial properties, however, method B allows for easier determination of the droplet shape, thereby enabling estimates of interfacial and surface tensions. The average interfacial tension between slag and metal over the temperature interval was found to be 1.08±0.10 N/m for S/M 0.19, and 1.30±0.32 N/m for S/M 0.28, whereas the surface tension of slag in Ar is 1.13±0.52 N/m for S/M 0.19, and 1.10±0.30 N/m for S/M 0.28. Both interfacial and surface tension was found to decrease slightly with increasing temperature. Moreover, it has been observed that both methods are

sensitive to the slag-to-metal ratio, which modifies the gravity effect and therefore the force balance in the system. Future work aims to improve the processing procedure so that the true tensions can be determined from the apparent values presented here as well as taking actions to reduce the uncertainty in measurements.

REFERENCES

1 *World Steel in Figures 2018*, World Steel Association, 2018.
2 C. Bories: *2018 Results*, Eramet, 2019.
3 A. Figueiredo, A. Werner, C.A. Miller, F. Mascarenhas, S. Bassil, B. Siqueira, C. Couri, and R. Capanema: *Vale's Production and Sales in 3Q18*, Investor Relations Department, Vale, 2018.
4 *IMnI Statistics 2018*, International Manganese Institute, 2018.
5 *2015 Minerals Yearbook, Ferroalloys [Advance Release]*, U.S. Department of the Interior, U.S. Geological Survey, 2018.
6 A.V. Zhdanov, V.I. Zhuchkov, V.Y. Dashevskiy, and L.I. Leontyev: in *Advanced Methods and Technologies in Metallurgy in Russia*, S. Syngellakis and J.J. Connor, eds., Springer International Publishing, Cham, 2018, pp. 113–20.
7 L.R. Nelson and R.J. Hundermark: *J. South. Afr. Inst. Min. Metall.*, 2016, vol. 116, pp. 465–90.
8 M. Kadkhodabeigi: Modeling of Tapping Processes in Submerged Arc Furnaces, NTNU, 2011.
9 H.-S. Jang, J.W. Ryu, and I. Sohn: *Metall. Mater. Trans. B*, 2015, vol. 46, pp. 606–14.
10 G. Irons, A. Senguttuvan, and K. Krishnapisharody: *ISIJ Int.*, 2015, vol. 55, pp. 1–6.
11 A.F. Yang, A. Karasev, and P.G. Jönsson: *ISIJ Int.*, 2015, vol. 55, pp. 570–7.
12 Z. Han and L. Holappa: *ISIJ Int.*, 2003, vol. 43, pp. 292–7.
13 L. Muhmood, N.N. Viswanathan, and S. Seetharaman: *Metall. Mater. Trans. B*, 2011, vol. 42, pp. 460–70.
14 T. Tanaka, H. Goto, M. Nakamoto, M. Suzuki, M. Hanao, M. Zeze, H. Yamamura, and T. Yoshikawa: *ISIJ Int.*, 2016, vol. 56, pp. 944–52.
15 M. Tangstad: *Handbook of Ferroalloys: Chapter 7. Manganese Ferroalloys Technology*, Elsevier Inc. Chapters, 2013.
16 J. Muller, J.H. Zietsman, and P.C. Pistorius: *Metall. Mater. Trans. B*, 2015, vol. 46, pp. 2639–51.
17 C.A. Schneider, W.S. Rasband, and K.W. Eliceiri: *Nat. Methods*, 2012, vol. 9, pp. 671–5.
18 S.M.I. Saad and A.W. Neumann: *Adv. Colloid Interface Sci.*, 2016, vol. 238, pp. 62–87.
19 P. Morel: Gramm, http://joss.theoj.org, (accessed 25 March 2019).
20 S. Bao, K. Tang, A. Kvithyld, M. Tangstad, and T.A. Engh: *Metall. Mater. Trans. B*, 2011, vol. 42, pp. 1358–66.
21 K. GmbH: *Effect of Drop Volume on Static Contact Angles*, 2004.
22 V.V. Kashin, K.M. Shakirov, and A.I. Poshevneva: *Steel Transl.*, 2011, vol. 41, pp. 795–8.
23 A. Calvimontes: DOI:10.20944/preprints201708.0062.v2.
24 Hondros E. D., McLean M., Mills K. C., Hibiya Taketoshi, Nakamura Shin, Mukai Kusuhiro, Niu Zheng–Gang, Imaishi Nobuyuki, Nishizawa Shin–ichi, Yoda Shin–ichi, and Koyama Masato: *Philos. Trans. R. Soc. Lond. Ser. Math. Phys. Eng. Sci.*, 1998, vol. 356, pp. 899–909.
25 R. Brooks, I. Egry, S. Seetharaman, and D. Grant: *High Temp.-High Press.*, 2001, vol. 33, pp. 631–7.
26 M. Wegener, L. Muhmood, S. Sun, and A.V. Deev: *Metall. Mater. Trans. B*, 2015, vol. 46, pp. 316–27.
27 L. Muhmood, N.N. Viswanathan, and S. Seetharaman: *Metall. Mater. Trans. B*, 2011, vol. 42, pp. 460–70.
28 E.-J. Kim, B.-D. You, and J.-J. Pak: *Metall. Mater. Trans. B*, 2003, vol. 34, pp. 51–9.